International Journal of Modern Physics B
Vol. 23, No. 20 & 21 (2009) 3951–3967
© World Scientific Publishing Company

World Scientific
www.worldscientific.com

Int. J. Mod. Phys. B 2009.23:3951-3967. Downloaded from www.worldscientific.com
by SIMON FRASER UNIVERSITY on 02/02/15. For personal use only.

2D ISING MODEL WITH COMPETING INTERACTIONS AND ITS APPLICATION TO CLUSTERS AND ARRAYS OF π-RINGS, GRAPHENE AND ADIABATIC QUANTUM COMPUTING

ANTHONY O'HARE

Department of Physics, Loughborough University, Leicestershire, LE11 3TU, UK.

F. V. KUSMARTSEV

Department of Physics, Loughborough University, Leicestershire, LE11 3TU, UK.

K. I. KUGEL

Institute for Theoretical and Applied Electrodynamics, Russian Academy of Sciences, Izhorskaya Str. 13, Moscow, 125412 Russia

Received 24 July 2009

We study the two-dimensional Ising model with competing nearest-neighbour and diagonal interactions and investigate the phase diagram of this model. We show that the ground state at low temperatures is ordered either as stripes or as the Néel antiferromagnet. However, we also demonstrate that the energy of defects and dislocations in the lattice is close to the ground state of the system. Therefore, many locally stable (or metastable) states associated with local energy minima separated by energy barriers may appear forming a glass-like state.

We discuss the results in connection with two physically different systems. First, we deal with planar clusters of loops including a Josephson π-junction (a π-rings). Each π-ring carries a persistent current and behaves as a classical orbital moment. The type of particular state associated with the orientation of orbital moments in the cluster depends on the interaction between these orbital moments and can be easily controlled, i.e. by a bias current or by other means. Second, we apply the model to the analysis of the structure of the newly discovered two-dimensional form of carbon, graphene. Carbon atoms in graphene form a planar honeycomb lattice. Actually, the graphene plane is not ideal but corrugated. The displacement of carbon atoms up and down from the plane can be also described in terms of Ising spins, the interaction of which determines the complicated shape of the corrugated graphene plane.

The obtained results may be verified in experiments and are also applicable to adiabatic quantum computing where the states are switched adiabatically with the slow change of coupling constant.

Keywords: Ising model; transfer matrix; frustrations; superstructures; phase diagram; glassy state; arrays of Josephson π-rings; graphene; adiabatic quantum computer.

Int. J. Mod. Phys. B 2009.23:3951-3967. Downloaded from www.worldscientific.com
by SIMON FRASER UNIVERSITY on 02/02/15. For personal use only.

1. Introduction

In a large number of low-dimensional magnets, not only nearest neighbor interactions but also next-nearest neighbor ones play an important role. If the nearest-neighbor coupling constant J is positive, in the absence of the next-nearest-neighbor bonds ($J' = 0$), the system is a simple antiferromagnet on bipartite lattices (e.g., a square lattice in 2D). The turning on next-nearest-neighbor coupling of the same sign ($J' > 0$) leads to the frustration. The effects related to the interplay between frustration and quantum fluctuations in 2D quantum spin systems were actively studied in the recent years both theoretically (see, e.g., Refs. 1, 2, 3, 4, 5, 6, 7, 8, 9, 10 and references therein) and experimentally[21,22]. These effects can lead to quantum phase transitions between magnetically ordered semiclassical and novel quantum paramagnetic ground-state phases such as glasses, whose nature and order parameter may be very non-trivial.

A vivid example of such a system is given by planar clusters consisting of loops including a Josephson π-junction (π-rings). A single π-ring is a superconducting loop consisting of Josephson junctions where at least one of them is a π-junction[19]. Recently π-rings made of a combination of different, high-temperature and low-temperature, superconducting materials were deposited onto substrates in the form of one-dimensional and two-dimensional arrays[17,23]. If there is one or an odd number of π-junctions in a loop, then the phase shift by π results in a doubly degenerate time-reversed ground states in the loop. Thus, a persistent supercurrent circulating in a clockwise or counter-clockwise direction[19] appears. Therefore, a phase shift by π in such a junction results in the formation of an orbital current or a magnetic moment at the ring (see[19] for details). This means that a π-ring has the possibility of being used as a qubit.

A chain or a planar array of electrically isolated π-rings could be treated as a set of magnetic moments oriented perpendicular to the plane (Ising spins) and interacting via magnetic dipole forces (in this geometry these interactions will have an antiferromagnetic sign). Due to this dipole character of the interaction between the orbital moments, it is necessary to include the next-nearest neighbor interactions in addition to those between the nearest neighbors in the model. This dipole-dipole interaction may modify the values of the orbital magnetic moments and leads to a formation of the disordered and/or fractal structures in a one-dimensional chain[18].

The ground state of a π-ring cluster depends on the coupling between the π-rings. Varying the couplings, one can obtain different ground states. For the conventional planar array of π-rings studied, for example, in Ref. 17, the interaction between the individual π-ring is mainly of the dipole-dipole character and fixed. However, an introduction of additional Josephson junction or a current loop located between the π-rings or other Josephson loops with persistent current may change this coupling significantly. For example, an introduction of an additional Josephson junction between two flux qubits, each consisting of three Josephson junctions formed a well controllable coupling between these qubits[20].

Int. J. Mod. Phys. B 2009.23:3951-3967. Downloaded from www.worldscientific.com
by SIMON FRASER UNIVERSITY on 02/02/15. For personal use only.

Another interesting realization of the 2D Ising model with competing interactions could be related to graphene - a 2D crystalline layer of carbon atoms forming a honeycomb lattice. However, strictly speaking, the ideal 2D crystal cannot exist. There will always arise an instability, which can lead to a breakdown of the ideal planar configuration. Here, we show that this instability leads to a buckling in the planar system. Such type of buckling was earlier observed for silicon surfaces and was studied in a framework of different Ising-type models, which are always associated with the symmetry of the underlying lattices. There, the Ising spin variables correspond to an out-of-plane shift of silicon atoms. Following the same approach here, we describe the buckling of graphene by the Ising model with competing interactions where the transverse shift of carbon atoms out of the plane (breaking the planar symmetry) is associated with up and down Ising spins. Based on this model, we demonstrate that with a decrease in temperature, there first arises a conventional order-disorder transition. The ordered state is associated with stripes of carbon atoms shifted to one or another directions with respect to the plane. However, there are striking features at lower temperatures, where this order disappears and is replaced by a glassy state. At such low temperatures this glassy state may produce a pronounced effect on electronic transport in graphene.

2. The Model (Square Lattice)

We start from the two-dimensional Ising model with antiferromagnetic nearest-neighbor and diagonal interactions. The Hamiltonian for such a model can be written as

$$H = J \sum_{\langle i,j\rangle_{nn}} s_i s_j + J' \sum_{\langle i,j\rangle_{dn}} s_i s_j - h \sum_i s_i \tag{1}$$

Here $J, J' > 0$, s is a two-value Ising variable, $s = \pm 1$, $\langle i,j\rangle_{nn}$ and $\langle i,j\rangle_{dn}$ denote the summation over sites i and j being respectively nearest neighbors (nn) and diagonal neighbors (dn), and h is the magnetic field in energy units (we will ignore the magnetic field in the discussion throughout this paper). The geometry of the model is schematically illustrated in Fig. 1.

Let us begin by rewriting the Hamiltonian 1 for the $N \times N$ square lattice as

$$H = \sum_{j=1}^{N} \Big[E(\mu_j, \mu_{j+1}) + E(\mu_j) \Big] \tag{2}$$

where the summation is over all possible configurations, j, and the terms $E(\mu_j, \mu_{j+1})$ and $E(\mu_j)$ are given by

$$\begin{aligned} E\left(\mu_j, \mu_k\right) &= J \sum_{i=1}^{N} \sigma_{i,j}\sigma_{i,k} + J' \sum_{i=1}^{N} \left(\sigma_{i,j}\sigma_{i+1,k} + \sigma_{i+1,j}\sigma_{i,k}\right) \\ E(\mu_j) &= J \sum_{i=1}^{N} \sigma_{i,j}\sigma_{i+1,j} - h \sum_{i=1}^{N} \sigma_{i,j} \end{aligned} \tag{3}$$

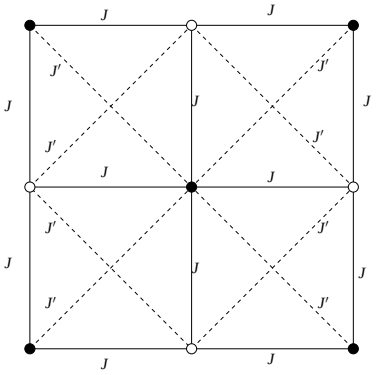

Fig. 1. Ising model with nearest neighbor J and diagonal J' interactions for the square lattice. Filled and open circles mean $s = +1$ and $s = -1$, respectively. Here, the usual two-sublattice arrangement of spins is shown.

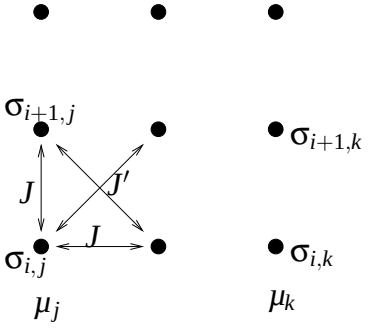

Fig. 2. Interactions between lattice columns in the 2D Ising model with next-nearest neighbor interactions that define the transfer matrix.

Here, μ_j denotes the set of spins in a column of the lattice $\mu_j \equiv \{\sigma_{1,j}, \sigma_{2,j} \ldots \sigma_{N,j}\}$. We can visualise the interactions between sites as in Fig. 2.

We can now define the following $2^N \times 2^N$ matrix for Hamiltonian 2

$$\langle \mu_j | M | \mu_k \rangle = \exp\left(-\beta \left[E(\mu_j \mu_k) + E(\mu_j)\right]\right) \tag{4}$$

Using this form of the Hamiltonian, we can write the partition function, which is in fact a generalization of the well-known partition function for the 2D Ising model with nearest neighbor interactions ($\beta = 1/k_B T$)

$$\begin{aligned} Z(\mathcal{H}, \beta) &= \sum_{\mu_1} \cdots \sum_{\mu_N} \exp\{-\beta \sum_{j=1}^{N} \left[E\left(\mu_j, \mu_{j+1}\right) + E\left(\mu_j\right)\right] \\ &= \sum_{\mu_1} \cdots \sum_{\mu_N} \langle \mu_1 | \mathbf{T} | \mu_2 \rangle \langle \mu_2 | \mathbf{T} | \mu_3 \rangle \ldots \langle \mu_N | \mathbf{T} | \mu_1 \rangle \\ &= \sum_{\mu_1} \langle \mu_1 | \mathbf{T}^N | \mu_1 \rangle \end{aligned} \tag{5}$$

Int. J. Mod. Phys. B 2009.23:3951-3967. Downloaded from www.worldscientific.com
by SIMON FRASER UNIVERSITY on 02/02/15. For personal use only.

Here $\mathbf{T}$ is the transfer matrix. The partition function, $Z(\mathcal{H}, \beta)$, is a matrix product. Performing this product corresponds to calculating the trace over $\mathbf{T}$.

$$Z(\mathcal{H}, \beta) = \mathbf{Tr}\mathbf{T}^N \tag{6}$$

which can be shown to be

$$Z(\mathcal{H}, \beta) = \mathbf{Tr}(\mathbf{T}^N) = \lambda_0^N \tag{7}$$

where λ_0 is the eigenvalue with the largest modulus.

3. Phase Diagram

The free parameters in the transfer matrix are the ratio of exchange constants, J/J', and the temperature, T so we can create the transfer matrix at each value of $(J/J', T)$. We calculate the eigenvalue with the largest modulus at each point of the $(J/J', T)$ space and the free energy ($\mathcal{F} = -k_B T N \log \lambda_0$) and differentiate this (numerically) to obtain the specific heat the peaks of which are used to determine the phase diagram of the system.

The results are presented in Fig. 3. One can see there well-defined broad peaks, which have the lowest height in the parameter range, where the ratio $J/J' \sim 2$. This is exactly the range, where the frustration is the largest. Obviously, these peaks are associated with the order-disorder phase transition.

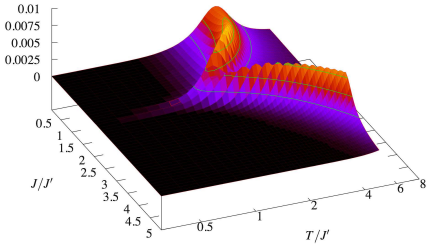

Fig. 3. Specific heat for the for the Ising model with next-nearest neighbor interactions on an 8×8 lattice calculated using the transfer matrix method.

We can see that there are three distinct regions in the phase diagram, a high-temperature phase and two low-temperature phases separated by $J/J' = 2$. For $J/J' < 2$ we can see that stripe ordering is favorable while the Néel antiferromagnetic (checkerboard) ordering is favorable for $J/J' > 2$. For $J/J' = 2$, we have a crossover from stripe to checkerboard antiferromagnetic ordering. This crossover could exist over a larger range of J/J'; in practice where it would manifest itself by the formation of domains with either stripe or antiferromagnetic Néel-type ordering.

In Fig. 4, we show the phase diagram of the Hamiltonian investigated in the present paper and compare it with the phase diagram from Monte Carlo simulations.

Int. J. Mod. Phys. B 2009.23:3951-3967. Downloaded from www.worldscientific.com
by SIMON FRASER UNIVERSITY on 02/02/15. For personal use only.

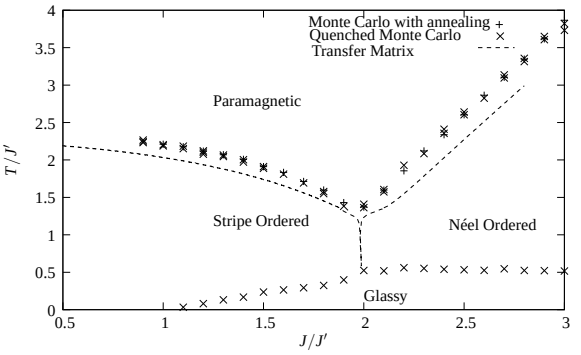

Fig. 4. Phase diagram for the Ising model with next-nearest neighbor interactions. The peaks in the specific heat were used to determine the location of the phase transition. The phase diagram has been compared with Monte Carlo simulations on an 8×8 lattice where a low-temperature glass-like phase is seen.

4. Low-Temperature Glassy State

In Fig. 4, we see that the specific heat data provided by the Monte Carlo simulations provide a compelling evidence of the low-temperature glassy state. However, the exact solution obtained by the transfer matrix method in previous section does not provide a direct evidence for such a glassy state. Although we found that in the area of the phase diagram associated with the glassy state the largest eigenvalues become degenerate, it is still not clear how to express this finding in the form of the order parameter. Let us discuss this issue in more detail.

Here, we introduce a simple and transparent method allowing us to analyze the properties of a glass-like phase, which may reflect the appearance of the degeneracy in the transfer matrix spectrum. The glassy state is treated as a set of small domains separated by domain boundaries. In such an approach, the length of domain boundaries can be considered as a measure of the "glassiness" of the system.

First of all, let us introduce a non-standard definition of a domain boundary as a topological defect, which could help us in the further numerical analysis of the glassy state. Of course, arguing that the domain boundary is a topological defect, we should first define the ordered state. It is natural to start with the usual two-sublattice ordering of Ising spins, where each site of one sublattice is surrounded by the sites of the other sublattice with the spins of opposite direction. Then, we can define a domain boundary as the boundary between two pieces of the ordered phase displaced with respect to each other. Hence, the uniform antiferromagnetic two-sublattice state has no domain boundaries. At the same time, the antiferromagnetic state with alternating ferromagnetic chains of opposite spins (horizontal or vertical stripes) may be treated as a state with maximally dense (with the period of one lattice constant) parallel domain boundaries.

Under such a definition of a domain boundary, we can also characterize an arbitrary disordered Ising state. For this purpose, let us introduce a measure of

Int. J. Mod. Phys. B 2009.23:3951-3967. Downloaded from www.worldscientific.com
by SIMON FRASER UNIVERSITY on 02/02/15. For personal use only.

the disorder associated with the domain boundary length l_d. The simplest way to do this is to normalize such length per one lattice site. Then the antiferromagnetic state with horizontal or vertical stripes should be treated as a state with the domain boundary length $l_d = 2$, whereas a classical two-sublattice antiferromagnetic Ising state will correspond to $l_d = 0$. Then, for an arbitrary disordered state, the mean normalized length should fall within the $0 < l_d < 2$ range. Probably, the maximum disorder will correspond to $l_d = 1$. Note, that at an applied magnetic field, the above inequality is violated. For example, in the saturated ferromagnetic state, we have $l_d = 4$.

In Figs. 5 and 6, we show the temperature dependence of the domain boundary length at different values of the J/J' ratio. The results depend on the method employed in the simulation, in the first (quenched) simulation we start with a random initial state and run the thermalising steps before taking measurements. We repeat the same steps for each temperature in the plot. In the annealing simulation we choose a random initial state for a high temperature, run the thermalising steps and take measurements. We then lower the temperature, keeping the state of the previous temperature at the end of the measurement steps as the initial state of the lower temperature. In this way, at low temperatures we always start our simulation in an ordered state in which the system remains. In the quenched simulation we see defects get "frozen" into the system at very low temperatures creating a cluster-glass state. In Fig. 5, we see that the quenched simulations exhibit a steep change in the mean length of domain walls at low temperatures. The corresponding onset temperature agrees well with that given by the low-temperature curve in Fig. 4.

The glassy state can be also analyzed in a more traditional way. Indeed, in a typical antiferromagnet at high temperature, the system exists in a paramagnetic state where the global magnetic moment, $m = \langle s_i \rangle$ is non-zero where there is a slight imbalance between the number of "up" and "down" spins and each spin is able to flip its orientation randomly. As the temperature is lowered the spins "freeze" in particular orientations so that the global magnetization becomes zero as antiferromagnetic ordering develops. At low temperatures, the system should exist in an ordered state with long-range order. However, randomness reduces correlations to a few spins, but temporal correlations due to freezing of the spins can be very strong. Local squared magnetisation is given by the average of the auto-correlation functions. This is the order parameter proposed by Edwards and Anderson[11].

$$q_{EA} = \lim_{t\to\infty} \lim_{V\to\infty} [\langle s_i(t_0) s_i(t_0 + t) \rangle]$$

Spin-glass ordering, if it can be described within the framework of equilibrium statistical mechanics, corresponds to a non-zero value of the Edwards-Anderson order parameter. We can see from Fig. 7 that Monte Carlo simulations clearly show the Edwards-Anderson order parameter exploding as $T/J' \to 0$. This is indicative of spin-glass ordering.

At the same time, when we use annealing to reach low temperatures we have a situation where, at low-temperatures, the system is in an ordered state (striped

Int. J. Mod. Phys. B 2009.23:3951-3967. Downloaded from www.worldscientific.com
by SIMON FRASER UNIVERSITY on 02/02/15. For personal use only.

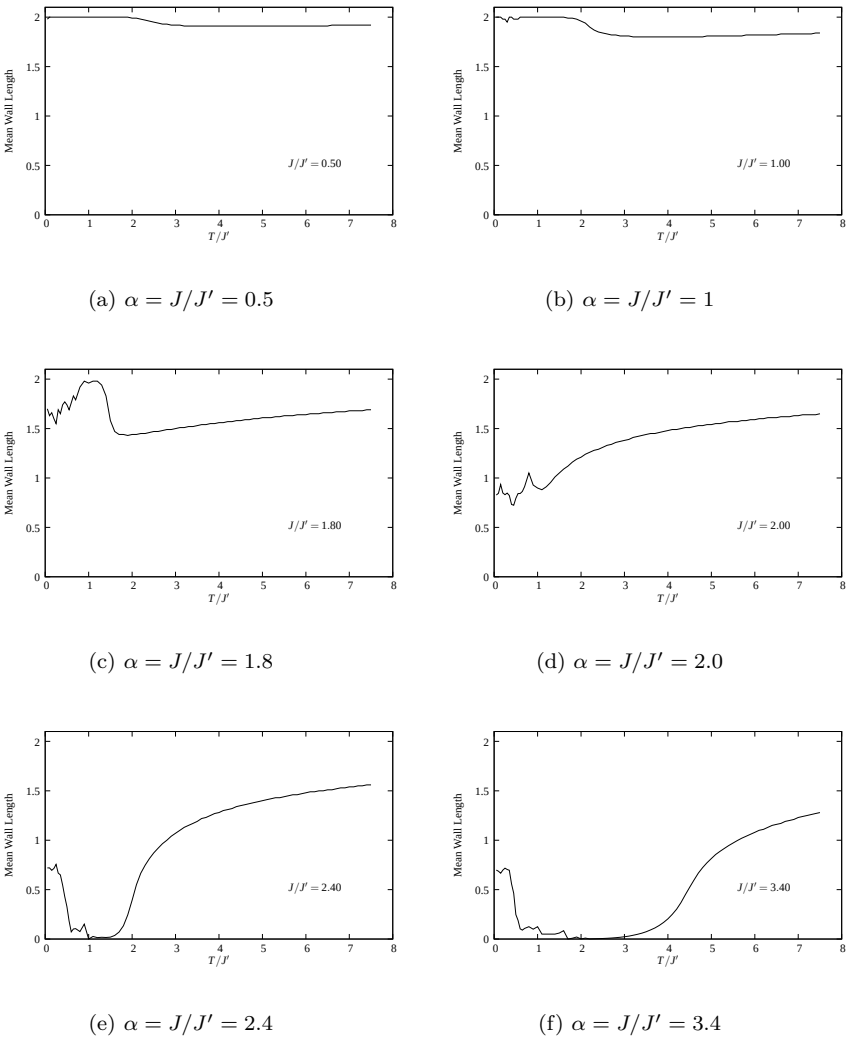

(a) $\alpha = J/J' = 0.5$ (b) $\alpha = J/J' = 1$

(c) $\alpha = J/J' = 1.8$ (d) $\alpha = J/J' = 2.0$

(e) $\alpha = J/J' = 2.4$ (f) $\alpha = J/J' = 3.4$

Fig. 5. Mean length of domain boundaries as function of temperature in the a 2D frustrated Ising model at different values of parameter $\alpha = J/J'$. The steep deviation of the mean length per lattice site from zero (at $\alpha > 2$) and from 2 (at $\alpha < 2$) is a signature of the onset of the glass-like state. Here, we present the results of Monte Carlo simulations without the annealing procedure (quenched system).

ordering at $J/J' < 2$ and antiferromagnetic ordering at $J/J' > 2$). If we were to anneal this system further, we would have a situation where the system is in an ordered ground state and where there is no energy available to create any frozen superstructures. This situation is illustrated in the right panel of Fig. 7.

Thus, different types of the Monte Carlo simulations reveal the existence of the low-temperature glass-like phase with quite unusual properties. The glassy state is

Int. J. Mod. Phys. B 2009.23:3951-3967. Downloaded from www.worldscientific.com
by SIMON FRASER UNIVERSITY on 02/02/15. For personal use only.

Int. J. Mod. Phys. B 2009.23:3951-3967. Downloaded from www.worldscientific.com
by SIMON FRASER UNIVERSITY on 02/02/15. For personal use only.

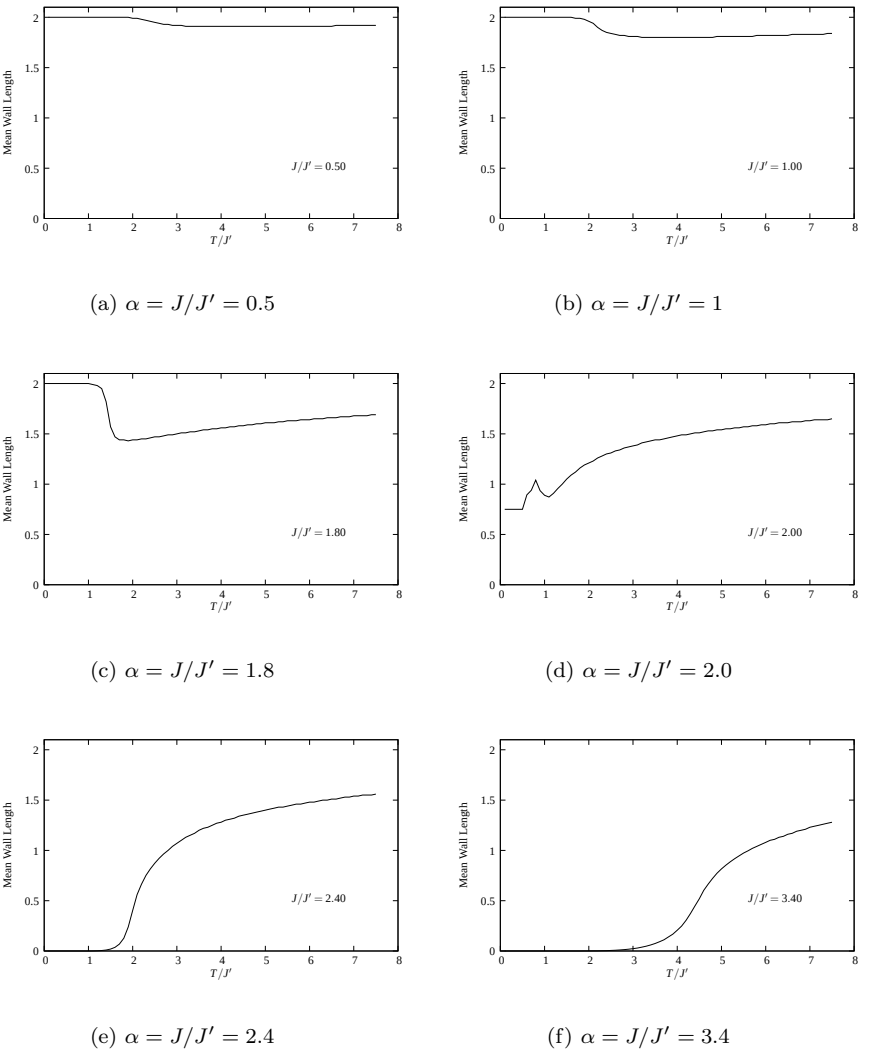

(a) $\alpha = J/J' = 0.5$ (b) $\alpha = J/J' = 1$

(c) $\alpha = J/J' = 1.8$ (d) $\alpha = J/J' = 2.0$

(e) $\alpha = J/J' = 2.4$ (f) $\alpha = J/J' = 3.4$

Fig. 6. Mean length of domain boundaries as function of temperature in the a 2D frustrated Ising model at different values of parameter $\alpha = J/J'$. The steep deviation of the mean length per lattice site from zero (at $\alpha > 2$) and from 2 (at $\alpha < 2$) is a signature of the onset of the glass-like state. Here, we present the results of Monte Carlo simulations with the annealing procedure (annealed system). Note that the annealing removes any signatures of low-temperature disorder, except for $\alpha < 2$, where the crossover between different types of the ground state occurs.

characterized by a proliferation of topological defects such as domain walls down to very low temperatures. That is why the appearance of the glassy state is well correlated with the change in the average length of domain walls, which play here a role of the order parameter for this glassy state.

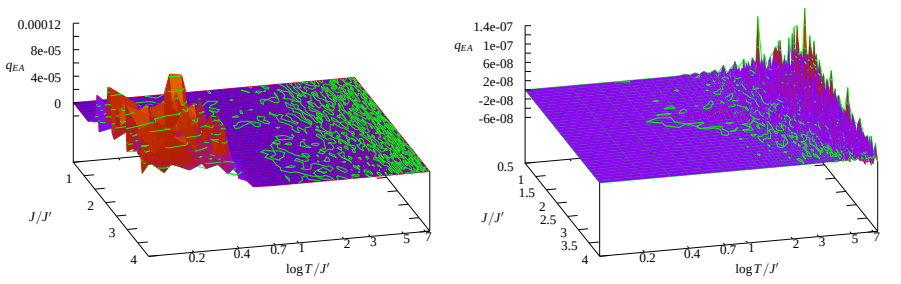

(a) (b)

Fig. 7. Edwards-Anderson order parameter for the 2D Ising model with next-nearest neighbor interactions on an 16×16 square lattice. The figure on the left is the result of Monte Carlo simulations while the one on the right is the result of a simulation using annealing. The explosion of the Edwards-Anderson order parameter at low temperature is an indication of the formation of a spin glass state, which only arises in the Monte Carlo simulation.

Let us now investigate these low-temperature superstructures. We write the radial correlation function as

$$\Gamma(r) = \langle s_i s_j \rangle - \langle s \rangle^2 \tag{8}$$

which measures the correlation between spins as a measure of the seperation between them. For a disordered system, we expect this function to decay rapidly as the separation increases. Figures 8, 9 show the radial correlation function for our Hamiltonian at $J/J' = 1.5$ and 3.0 (in the stripe and antiferromagnetic ordered regimes) respectively.

As we expect at high temperatures ($T.J' = 4.0$ in fig. 8) we see very little correlation due to the disorder of the system. At $T/J' = 1.0$, where the system exhibits stripe ordering we see very good long range ordering. In this case, since the spins are antialigned the correlation functions fluctuate between ± 1 as we extend through the lattice. Nevertheless the ordering is still long range. We would expect this long range ordering to extend to the lowest temperature but we see that this is not the case. A proliferation of defects in the lattice restricts ordering to only a few lattice spacings. However, there appears some non-zero long range correlation, the nature of which remains unclear.

This situation is repeated in the area of the phase diagram where we have Néel antiferromagnetic ordering. At low temperatures we have a proliferation of defects that restrict correlations to only a few lattice spacings.

5. Adiabatic Quantum Computing

The formation of a disordered glass-like state at low temperature may be utilised to perform adiabatic quantum computing. The idea is to prepare the system so that

Int. J. Mod. Phys. B 2009.23:3951-3967. Downloaded from www.worldscientific.com
by SIMON FRASER UNIVERSITY on 02/02/15. For personal use only.

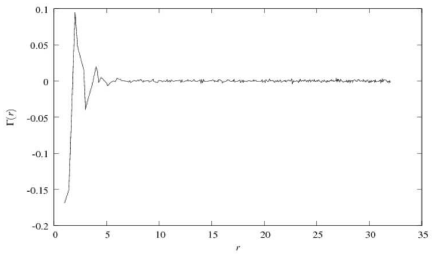

(a) $T/J' = 4.0$

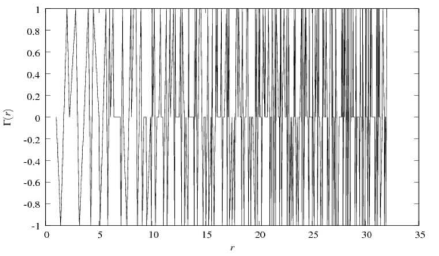

(b) $T/J' = 1.0$

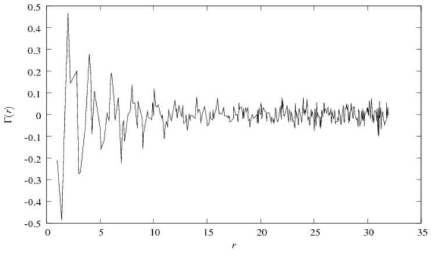

(c) $T/J' = 0.1$

Fig. 8. Radial correlation function at $J/J' = 1.5$.

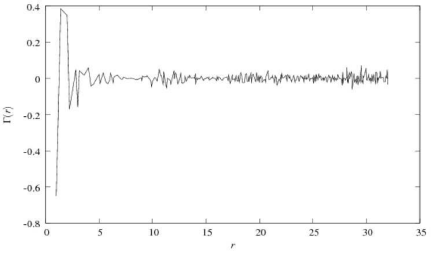

Fig. 9. Radial correlation function at $J/J' = 3.0$, $T/J' = 0.2$.

it is trapped in this glass-like state and thus may be used as an initial state for adiabatic quantum computing[13]. Thus, the system has a great capacity of states, which could be used in adiabatic quantum computations.

Recently, a scalable design has been proposed and realized that may be used in such a way[14] though the range of problems that may be solved may be limited. One such application is a Traveling Salesman Problem[15], which can be represented in the form of more complicated Ising model, with a set of a coupling constants[16].

Int. J. Mod. Phys. B 2009.23:3951-3967. Downloaded from www.worldscientific.com
by SIMON FRASER UNIVERSITY on 02/02/15. For personal use only.

Int. J. Mod. Phys. B 2009.23:3951-3967. Downloaded from www.worldscientific.com
by SIMON FRASER UNIVERSITY on 02/02/15. For personal use only.

6. Honeycomb Lattice: Application to Graphene

Let us now discuss, one more realization of the 2D Ising model, namely, graphene, a 2D modification of carbon attracting now a widespread attention[24]. While the ideal planar structures may exist for carbon monolayers deposited onto different substrates, now much effort is is focused on a freely suspended graphene films. However, such films exhibit different kinds of distortions in the location of carbon atoms, which were observed in recent experiments[25]. The experiments demonstrate that the distortions are mainly due to a displacement of carbon atoms out of the plane. Such displacements are obviously correlated due to elastic interactions between carbon atoms. Here, we show that these displacements of carbon atoms and associated elastic energy can be described in terms of the Ising model and Ising variables.

As we have already mentioned before, a purely 2D crystal is unstable. However, it can be stabilized by involving, at least partially, some kind of three-dimensionality. For the honeycomb lattice of graphene, the simplest possibility is a transverse displacement of carbon atoms (up and down from the horizontal plane). It is quite natural to put such displacements into correspondence to the two-valued Ising spin variables, namely, $S = 1$ could describe an upward displacement of a carbon atom (spin up), whereas $S = -1$ (spin down) could correspond to the downward displacement. To create a three-dimensionality, these upward and downward displacements should alternate forming some antiferrodistorsive pattern. Note that the energy loss due to changing of interatomic distance (elastic term) could be compensated by a larger hybridization of p orbitals of neighbouring carbon atoms[26]. Introducing the interactions between the displacements leads straightforwardly to the Ising model with the positive (antiferromagnetic) interaction constant. The origin of this Ising interaction is the elastic strain energy for neighbouring carbon atoms in the graphene lattice. Of course, due to the theory of elasticity, we deal with rather a long-range interaction and therefore we have to take into account at least the interaction between the next-nearest neighbours. As a result, we arrive at the following two-dimensional Ising model on the honeycomb lattice with the Hamiltonian taking into account the competing antiferromagnetic nearest and next-neighbour interactions, which has the same form as Hamiltonian (1), where the analog of magnetic field h corresponds some external strain. The geometry of the model is schematically illustrated in Fig. 10. Because the deformation energy of each atomic distortion decreases as $\sim 1/r^3$ for the graphene the ratio J/J' should be equal to $J/J' = 3^{3/2}$

Let us consider now a general case of this model, that is, different phases arising at arbitrary values of J/J'. When the interaction between the nearest neighbours dominates ($J \gg J'$), the minimum energy corresponds to the antiferrodistorsive structure shown in the left panel of Fig. 11. The next-nearest-neighbour interaction leads to frustrations, and the possible structure favorable at small J/J' is illustrated in the right panel of Fig. 11. The crossover between these two structures occurs at $J/J' = 4$.

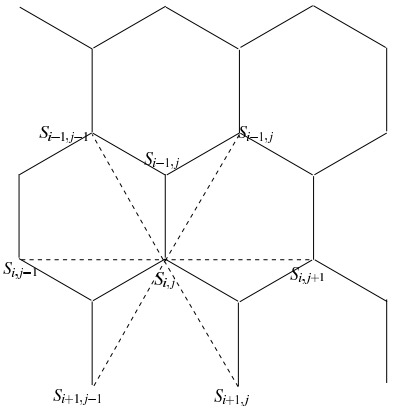

Fig. 10. Ising model with nearest neighbor J (solid lines) and diagonal J' (dashed lines) interactions for the honeycomb lattice.

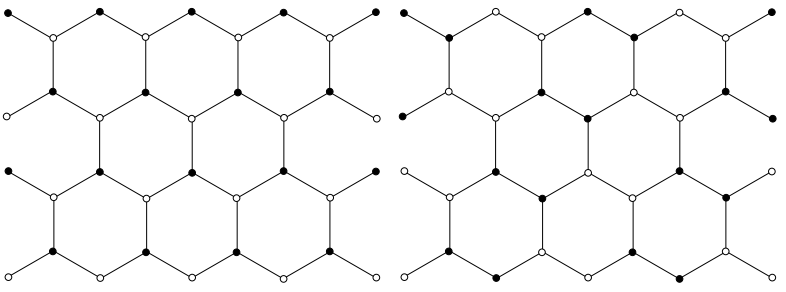

(a) $J > 4J'$ (b) $J < 4J'$

Fig. 11. Possible structures of Ising spins at the honeycomb lattice favorable in energy at large (a) and small (b) values of J/J' ratio.

In Fig. 12, we illustrate the evolution of the structure with temperature taken at $J/J' = 3^{3/2} \approx 5.2$ which ratio, we believe, is relevant for graphene. The latter value corresponds to the natural assumption that the coupling between distortions is inversely proportional to the cube the distance between them. The structures ("snapshots") were calculated by the Monte Carlo technique for 100×100 lattices.

The actual value of J/J' ratio in the graphene can vary in a vide range depending on applied stress, doping, etc., and may be controlled by external current or gate voltage. In Fig.12a, we see the pattern of atomic displacements formed at very low temperatures. We see from this figure that the system is in very disordered state. So, at low temperatures, there is a clear structure of domains walls and a proliferation of topological defects, while at high temperatures (0 Fig.12c) the disorder looks as a conventional one, i.e. it is difficult to identify there a clear domain structure. Between them, we see more or less regular structure corresponding to Fig.11a.

Int. J. Mod. Phys. B 2009.23:3951-3967. Downloaded from www.worldscientific.com
by SIMON FRASER UNIVERSITY on 02/02/15. For personal use only.

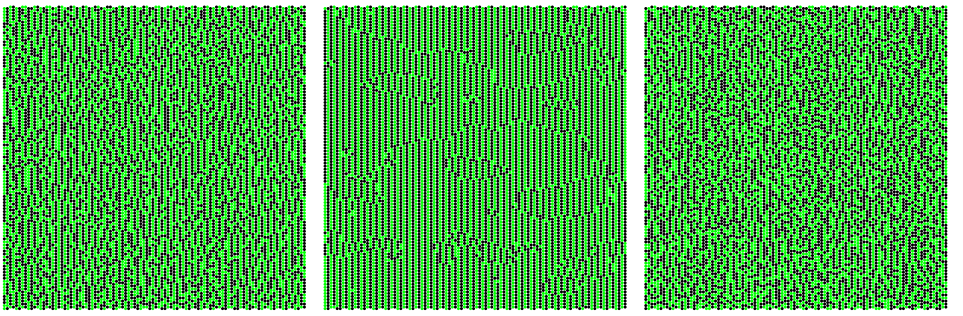

(a) $T/J' = 0.1$ (b) $T/J' = 2$ (c) $T/J' = 5.0$

Fig. 12. Snapshots of the superstructures formed on a honeycomb lattice with $J/J' = 3^{3/2}$ at various T/J'.

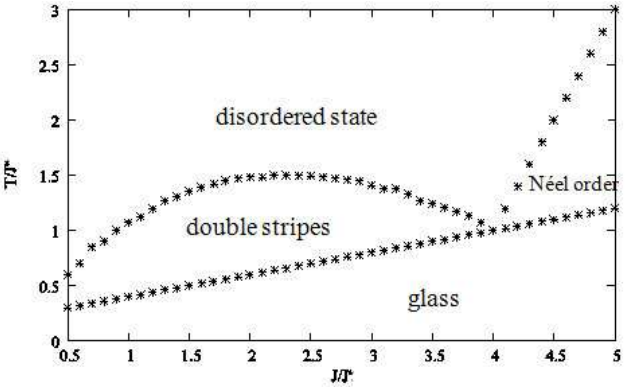

Fig. 13. Phase diagram for the model on a honeycomb lattice. The high temperature phase transition is calculated from the peaks in the specific heat while the low-temperature transition is obtained from the change in the magnetisation and the analysis of a domain-wall order parameter.

In Fig. 13, we present the phase diagram in $J/J' - T/J'$ plane calculated based on the Monte Carlo simulations and on the numerical solutions in the framework of the transfer matrix technique. Both methods give similar results that is there are two ordered or nearly states. One state is arising at the value $J/J' > 4$ at intermediate temperatures, i.e. when the value approximately within the range $J' < T < 2J'$. It is the conventional Néel antiferromagnetic ordering consisting of two triangular sublattices with ferromagnetic ordering (see Fig. 11a). The other ordered state is also arising at intermediate temperatures, i.e. approximately within the region $0.5J' < T < 1.5J'$, and when the value of the parameter $J/J' < 4$. In this case, there will arise the double-stripe ordering (see Fig. 11b). The phase diagram presented in Fig. 13 also indicates at low and at high temperatures at any ratio

Int. J. Mod. Phys. B 2009.23:3951-3967. Downloaded from www.worldscientific.com
by SIMON FRASER UNIVERSITY on 02/02/15. For personal use only.

J/J', a disordered state arises. At low temperatures, such state is presumably a glass, which is similar to the Ising glass described for the case of the square lattice.

At low temperatures, there is a clear structure of domains walls and a proliferation of topological defects, while at high temperatures the disorder looks as a conventional one, i.e. it is difficult to identify there a clear domain structure.

7. Conclusion

In summary, we described a formation of disordered state arising at very low temperatures. The disorder stems from a proliferation of topological defects. The striking point is that the disordered state is evolved from the ordered state when the temperature decreases. The cause of such behavior is related to a strong increase in the relaxation time for non-equilibrium domain walls when the temperatures decreases. Thus, with decreasing temperature, first, the ordered state is arising from a disordered state. This is a conventional, Ising, disorder-order phase transition. In the vicinity of this transition, in the ordered state, the relaxation time of the non-equilibrium domain walls is very short. Therefore, the topological defects vanish very fast. However, when temperature decreases, the height of the barriers separating the metastable minima associated with the domain walls increases. This leads to the exponential increase of the relaxation time of the non-equilibrium domain walls. In its turn, it leads to a formation of the disordered state associated with the remained domain walls and the glassy state arises. Because of the domain-wall nature, it is convenient to describe such glassy state with the use of the new order parameter associated with the average length of the domain walls existing in the system. Indeed, in the present paper, we have shown that such description is consistent with the conventional one, although there exists a less transparent description of the glassy state through the use of the Edwards-Anderson order parameter.

Obviously, such domain walls are always associated with metastable minima. Therefore, the zero value of entropy at low temperatures related to the state without domain walls, that is, consistent with the transfer matrix exact results presented in the paper. This fact indicates that the ground state for the square lattice at low temperatures is ordered either as stripes, $J/J' < 2$ or as the Néel antiferromagnet, $J/J' > 2$. However, the recent findings[12,13] in the framework of the model under study show that the energy of topological defects and dislocations in the lattice is very close to the ground state of the system. Therefore, many locally stable (or metastable) states associated with local energy minima separated by large energy barriers may appear forming a glass-like state.

Based on the Ising model for the honeycomb lattice, we also found that the strictly two-dimensional crystal of the graphene is unstable toward to a spontaneous breaking of the planar symmetry associated with a formation of a short-range microscopic structure. Such a structure is formed by a transverse displacement of the carbon atoms from the original crystal plane. At low temperatures, such displacements are randomly distributed and form a special type of glassy state - Ising glass.

Int. J. Mod. Phys. B 2009.23:3951-3967. Downloaded from www.worldscientific.com
by SIMON FRASER UNIVERSITY on 02/02/15. For personal use only.

. With increasing temperature the topological there arise an annealing of the topological defects and the antiferromagnetic ordered state arises. Due to a topological character of these defects the ordered state is never realised and with the further increase in temperature there arise another conventional Ising order-disorder transition at which the ordered antiferromagnetic state is transformed into the disordered state. The most important result of our studies is that the graphene films should exhibit microscopically ordered and disordered structures consisting of the transverse displacements. Such displacements make the shape of the graphene look as a lattice of cages. For example, in the case of the ordered state, each cage consists of a pairs, each consisting of the three carbon atoms shifted by about $1 - 2\mathring{A}$ with respect to each other. The existence of such cages may explain a high chemical activity of graphene and many other puzzling properties of the graphene observed recently.

Thus, different approaches to the analysis of the frustrated Ising model undertaken in our paper clearly and self-consistently with each other demonstrate the possibility of the remanent quenched disorder arising at low temperatures, which manifests itself as a glassy state. Careful preparation of the lattice could result in the system being trapped in this glass-like state which may be used as an initial state for adiabatic quantum computing[13]. Thus, the system has a great capacity of states, which could be used in adiabatic quantum computations.

Int. J. Mod. Phys. B 2009.23:3951-3967. Downloaded from www.worldscientific.com
by SIMON FRASER UNIVERSITY on 02/02/15. For personal use only.

Acknowledgments

The work was supported by the ESF network-program AQDJJ, European project CoMePhS, ISTC (grant G1335), and RFBR (project 08-02-00212).

References

1. P. Chandra and B. Doucot, Phys. Rev. B **38**, 9335 (1988).
2. E. Dagotto and A. Moreo, Phys. Rev. Lett. **63**, 2148 (1989).
3. J. Richter, Phys. Rev. B **47**, 5794 (1993). J. Richter, N.B. Ivanov, and K. Retzlaff, Europhys. Lett. **25**, 545 (1994).
4. R.F. Bishop, D.J.J. Farnell, and J.B. Parkinson, Phys. Rev. B **58**, 6394 (1998).
5. L. Capriotti, F. Becca, A. Parola and S. Sorella, Phys. Rev. Lett. **87**, 097201 (2001).
6. L. Siurakshina, D. Ihle and R. Hayn, Phys. Rev. B **64**, 104406 (2001).
7. T. Roscilde, A. Feiguin, A.L. Chernyshev, S. Liu and S. Haas, Phys. Rev. Lett. **93**, 017203 (2004).
8. J. Sirker, Z. Weihong, O. P. Sushkov, and J. Oitmaa, Phys. Rev. B **73**, 184420 (2006).
9. D. Schmalfusz, R. Darradi, J. Richter, J. Schulenburg, and D. Ihle, Phys. Rev. Lett. **97**, 157201 (2006).
10. J. Roberto Viana and J. Ricardo de Sousa, Phys. Rev. B **75**, 052403 (2007).
11. S.F. Edwards and P.W. Anderson, *J. Phys. F* **5**, 965 (1975).
12. A. O'Hare, F.V. Kusmartsev, M.S. Laad, and K.I. Kugel, Physica C **437-438**, 230 (2006).
13. A. O'Hare, F.V. Kusmartsev, K.I. Kugel, and M.S. Laad, Phys. Rev. B **76**, 064528 (2007).
14. V. Zakosarenko, N. Bondarenko, S.H.W. van der Ploeg, A. Izmalkov, S. Linzen, J. Kunert, M. Grajcar, E. Il'ichev, and H.-G. Meyer, Appl. Phys. Lett. **90**, 022501 (2007).

15. Tien D. Kieu, quant-ph/0601151.
16. Roman Martoňàk, Giuseppe E. Santoro, and Erio Tosatti, Phys. Rev. E **70**, 057701 (2004).
17. H. Hilgenkamp, Ariando, H.-J. H. Smilde, D. H. A. Blank, G. Rijnders, H. Rogalla, J. R. Kirtley, and C. C. Tsuei, Nature (London) **422**, 50 (2003).
18. F. V. Kusmartsev, D. M. Forrester, and M. S. Garelli, in *Physics of Superconducting Phase Shift Devices, Book of Abstracts*, ed. A. Barone et al., Ischia (Napoli), April 2–5, p. 21 (2005).
19. F.V. Kusmartsev, Phys. Rev. Lett. **69**, 2268 (1992).
20. S.H.W. van der Ploeg, A. Izmalkov, Alec Maassen van den Brink, U. Hübner, M. Grajcar, E. Il'ichev, H.-G. Meyer, and A.M. Zagoskin, Phys. Rev. Lett. **98**, 057004 (2007).
21. R. Melzi, P. Carretta, A. Lascialfari, M. Mambrini, M. Troyer, P. Millet, and F. Mila, Phys. Rev. Lett. **85**, 1318 (2000).
22. P. Carretta, N. Papinutto, C.B. Azzoni, M.C. Mozzati, E. Pavarini, S. Gonthier, and P. Millet, Phys. Rev. B **66**, 094420 (2002).
23. J. R. Kirtley, C. C. Tsuei, Ariando, H. J. H. Smilde, and H. Hilgenkamp, Phys. Rev. B **72**, 214521 (2005).
24. A. K. Geim, Science **324**, 1530 (2009).
25. J.C. Meyer, A. K. Geim, M. I. Katsnelson, K. S. Novoselov, T. J. Booth, and S. Roth, Nature **446**, 60 (2007).
26. A. H. Castro Neto, F. Guinea, N. M. R. Peres, K. S. Novoselov, and A. K. Geim, Rev. Mod. Phys. **81**, 109 (2009).

Int. J. Mod. Phys. B 2009.23:3951-3967. Downloaded from www.worldscientific.com
by SIMON FRASER UNIVERSITY on 02/02/15. For personal use only.